(Supporting Information)

Synthesis and reactions of a zirconium naphthalene complex bearing a tetraanionic C-capped triaryloxide ligand

Yusuke Nakanishi, Yutaka Ishida and Hiroyuki Kawaguchi*

Department of Chemistry, Tokyo Institute of Technology, Ookayama, Meguro-ku, Tokyo 152-8551, Japan

Contents

Synthesis of the benzyl complex $[K_2(thf)_2(O_3C)Zr(CH_2Ph)_2]$.
Reaction of the benzyl complex $[K_2(thf)_2(O_3C)Zr(CH_2Ph)_2]$ with Ph_3SiH_3.

Fig. S1 ^1H NMR spectrum of **2** in THF-d_8.
Fig. S2 $^{13}C\{^1H\}$ NMR spectrum of **2** in THF-d_8.
Fig. S3 ^1H NMR spectrum of **3** in THF-d_8.
Fig. S4 $^{13}C\{^1H\}$ NMR spectrum of **3** in THF-d_8.
Fig. S5 ^1H NMR spectrum of **4** in C_6D_6 at 343 K.
Fig. S6 $^{13}C\{^1H\}$ NMR spectrum of **4** in C_6D_6 at 343 K.
Fig. S7 ^1H NMR spectrum of **5** in THF-d_8.
Fig. S8 $^{13}C\{^1H\}$ NMR spectrum of **5** in THF-d_8.
Fig. S9 ^1H NMR spectrum of **6** in THF-d_8.
Fig. S10 $^{13}C\{^1H\}$ NMR spectrum of **6** in THF-d_8.
Fig. S11 ^1H NMR spectrum of $[K_2(thf)_2(O_3C)Zr(CH_2Ph)_2]$ in THF-d_8.
Fig. S12 $^{13}C\{^1H\}$ NMR spectrum of $[K_2(thf)_2(O_3C)Zr(CH_2Ph)_2]$ in THF-d_8.
Fig. S13 ^1H NMR spectrum of the reaction mixture of **2** with one equiv of Me_3SiN_3 after 1 h.
Fig. S14 ^1H NMR spectrum of the reaction mixture of **2** with one equiv of $MesN_3$ after 1 h.
Fig. S15 ^1H NMR spectrum of the reaction mixture of **2** with H_2 in THF-d_8 after 72 h.

Fig. S16 Molecular structure of **4**.
Fig. S17 Molecular structure of the benzyl complex $[K_2(O_3C)Zr(CH_2Ph)_2]$.

Table S1 Crystallographic data for **2**, **4**, **5**, and $[K_2(O_3C)Zr(CH_2Ph)_2]$.

Synthesis and structure of $[K_2(thf)_2(O_3C)Zr(CH_2Ph)_2]$.

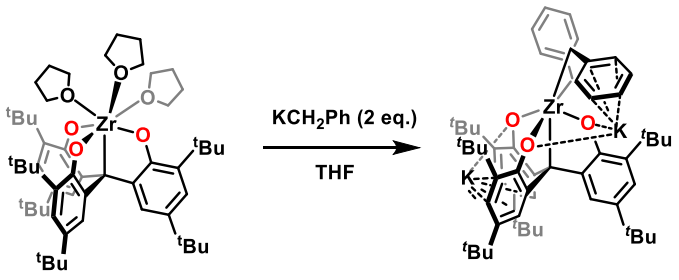

1

A solution of **1** (188 mg, 0.202 mmol) in toluene (15 mL) was slowly added to KCH_2Ph (53 mg, 0.41 mmol) in THF (10 mL) at –35 °C. The mixture was warmed to room temperature and stirred for 1h, and then all volatiles were removed in vacuo. The resulting residue was washed with toluene to give $[K_2(O_3C)Zr(CH_2Ph)_2]$ as a golden yellow powder in 77% (173 mg, 0.16 mmol). ^{1}H NMR (500 MHz, THF-d_8, rt, δ/ppm) 1.19 (s, 27H, ^{t}Bu), 1.40 (s, 27H, ^{t}Bu), 1.85 (s, 4H, – CH_2Ph), 6.26 (t, $^3J_{HH}$ = 6.9 Hz, 2H, – CH$_2$*Ph*), 6.74 (t, $^3J_{HH}$ = 6.9 Hz, 3H, – CH$_2$*Ph*), 6.80 (d, $^3J_{HH}$ = 6.9 Hz, 3H, – CH$_2$*Ph*), 6.88 (s, 3H, Ar), 7.16 (s, 3H, Ar). ^{13}C{^{1}H}NMR (125 MHz, THF-d_8, rt, δ/ppm) 30.9,32.2,34.5,35.5 (^{t}Bu), 57.6 (–*C*H$_2$Ph), 71.8 (Ar$_3$*C*Zr), 116.4,119.9, 125.4, 127.6, 127.7, 134.4, 144.0, 156.7, 163.9 (Ar). Anal. calcd (%) for $C_{57}H_{74}K_2O_3Zr$: C 70.10, H 7.64 ; found : C 70.52, H 7.68.

Reaction of the benzyl complex $[K_2(thf)_2(O_3C)Zr(CH_2Ph)_2]$ with Ph_3SiH_3.

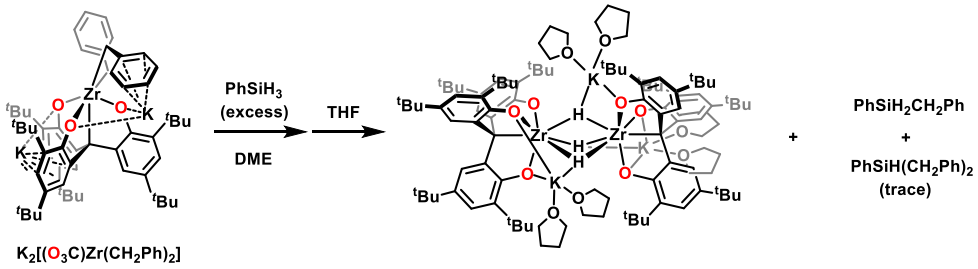

$K_2[(O_3C)Zr(CH_2Ph)_2]$ 6

To a solution of $[K_2(O_3C)Zr(CH_2Ph)_2]$ (46 mg, 0.041 mmol) in DME (2 mL) was added $PhSiH_3$ (12.0 μL, 0.097 mmol). The mixture was stirred at room temperature for 12h, during which time formation of a precipitation was observed. After centrifugation, the supernatant was decanted off and the remaining gray solid was extracted with 2 mL of THF. The solvent was removed in vacuo to leave **6** as pale yellow powder in 71% (29 mg, 0.015 mmol). ^{1}H NMR (500 MHz, THF-d_8, rt, δ/ppm) 1.28 (s, 27H, ^{t}Bu), 1.53 (s, 27H, ^{t}Bu), 4.70 (s, 3H, Zr–*H*), 6.83 (s, 3H, Ar), 7.33 (s, 3H, Ar). ^{13}C{^{1}H} NMR (125 MHz, THF-d_8, rt, δ/ppm) 30.6, 31.6, 33.8, 35.0 (^{t}Bu), 76.1 (Ar$_3$*C*Zr), 117.6, 126.7, 132.3, 136.9, 146.2, 166.0 (Ar). Anal. calcd (%) for $C_{110}H_{171}K_3O_{12}Zr_2$: C 66.55, H 8.68 ; found : C 65.71, H 8.24.

Fig. S1 ^{1}H NMR spectrum of **2** in THF-d_8.

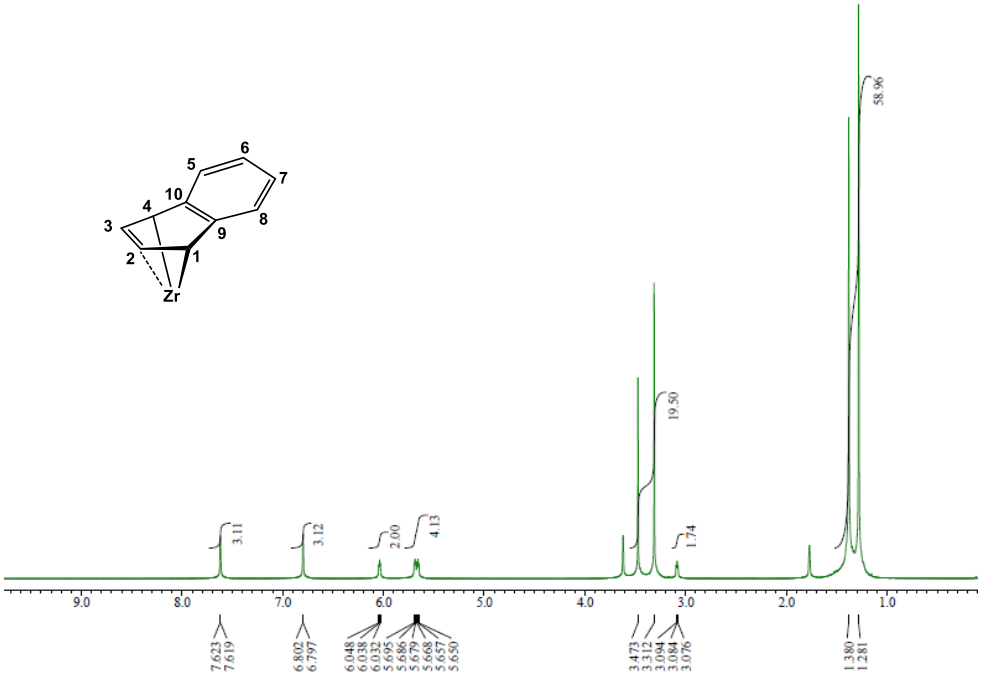

Fig. S2 ^{13}C{^{1}H} NMR spectrum of **2** in THF-d_8.

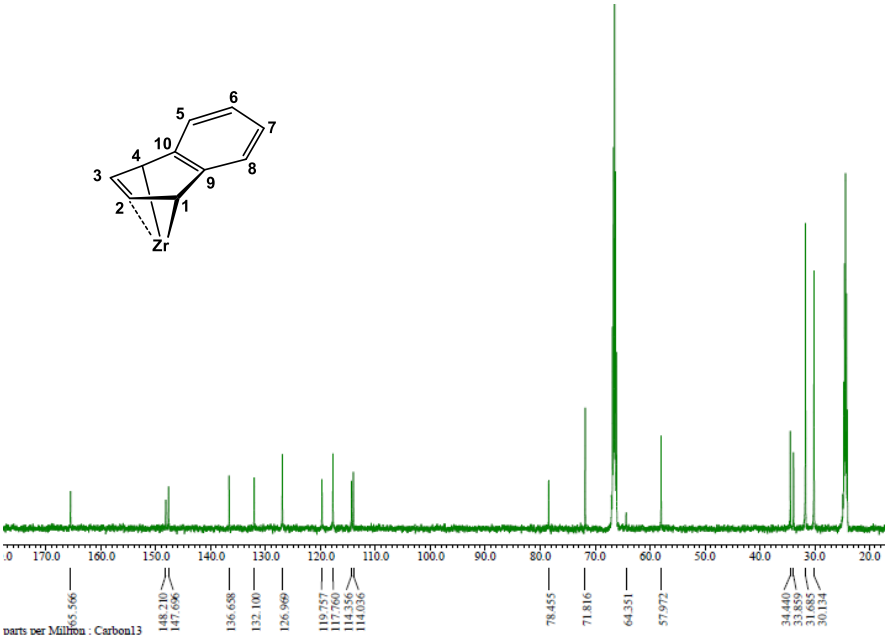

Fig. S3 ^{1}H NMR spectrum of **3** in THF-d_8.

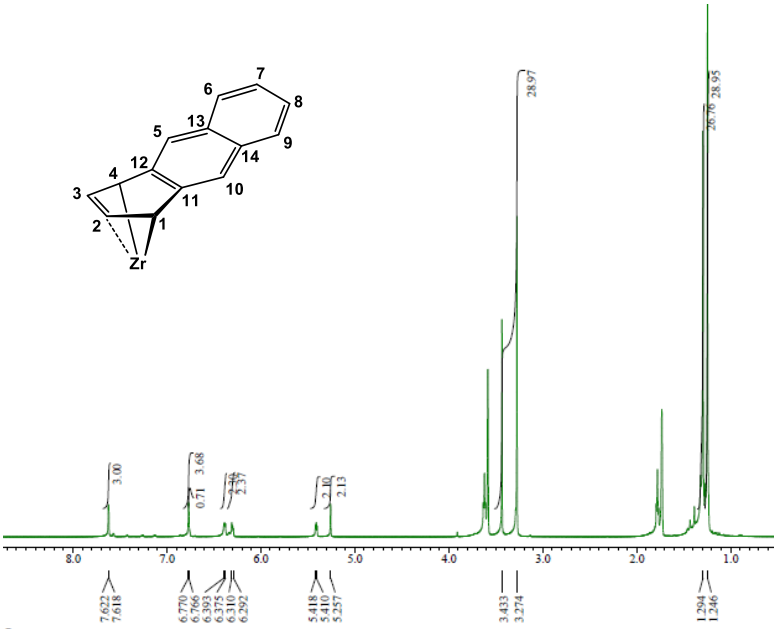

Fig. S4 ^{13}C{^{1}H} NMR spectrum of **3** in THF-d_8.

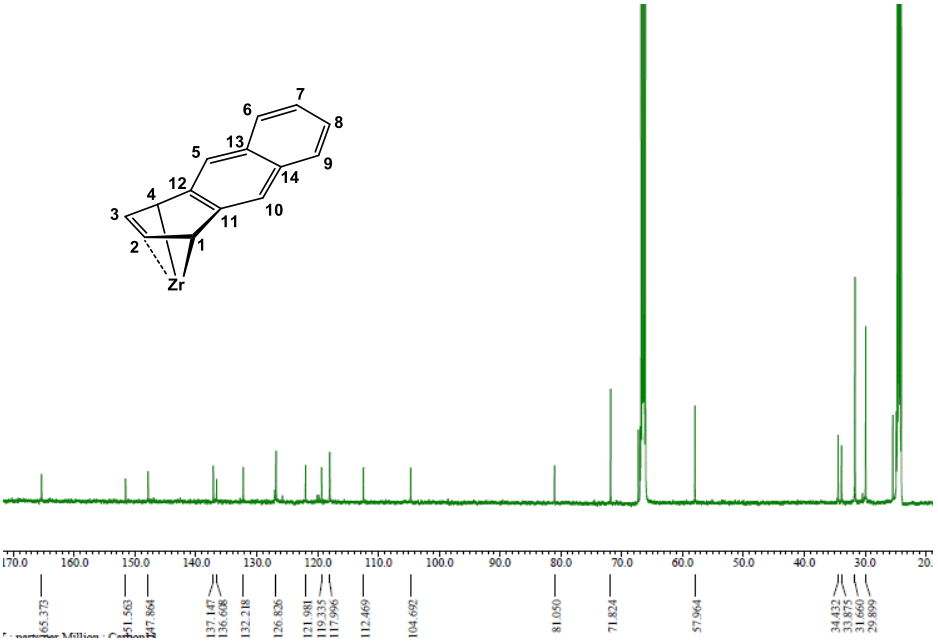

Fig. S5 ^{1}H NMR spectrum of **4** in C_6D_6 at 343 K.

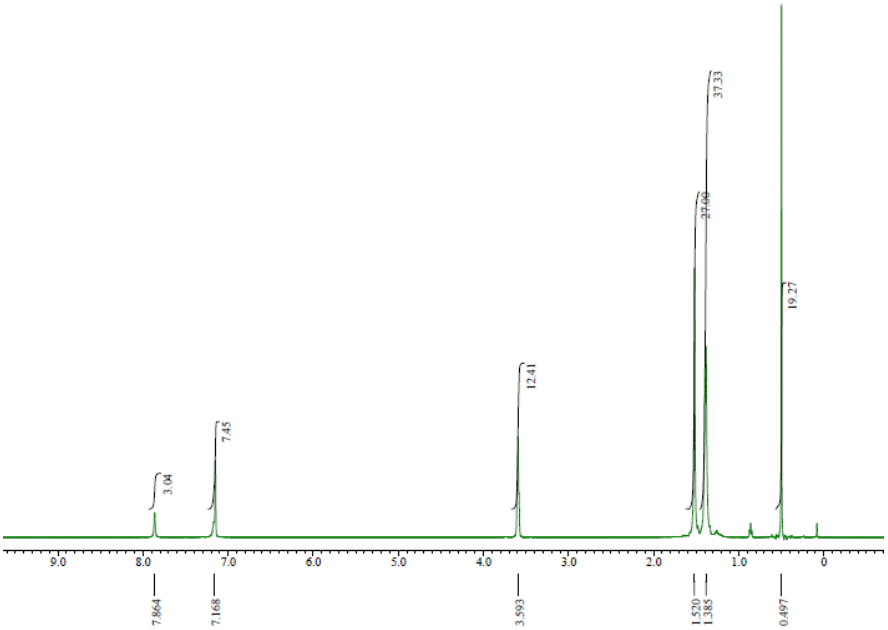

Fig. S6 $^{13}C\{^{1}H\}$ NMR spectrum of **4** in C_6D_6 at 343 K.

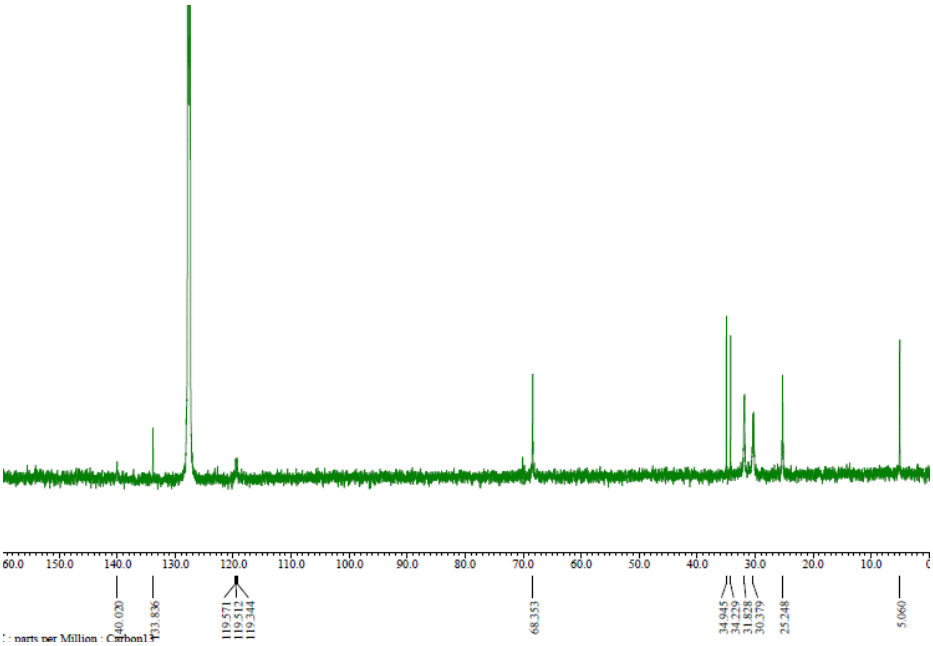

Fig. S7 ^{1}H NMR spectrum of **5** in THF-d_8.

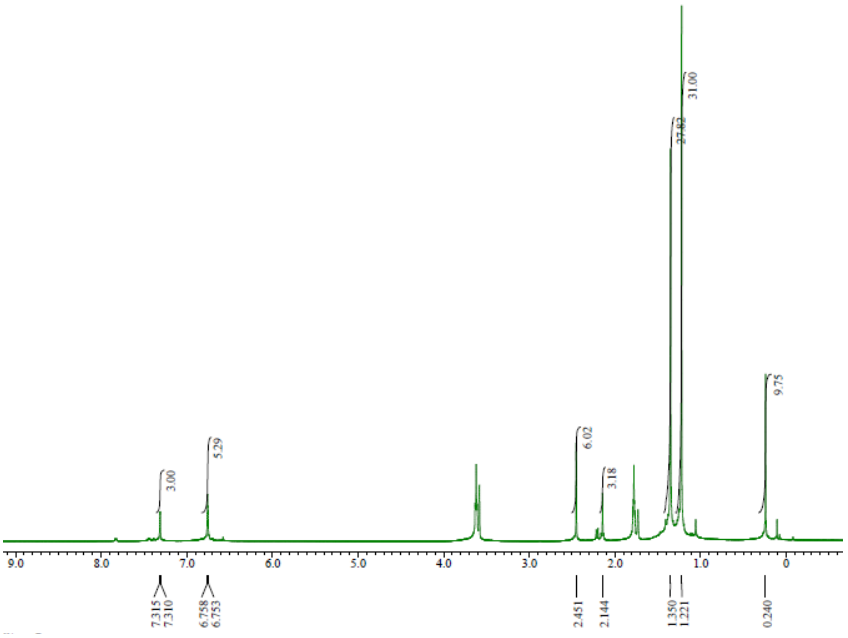

Fig. S8 ^{13}C{^{1}H} NMR spectrum of **5** in THF-d_8.

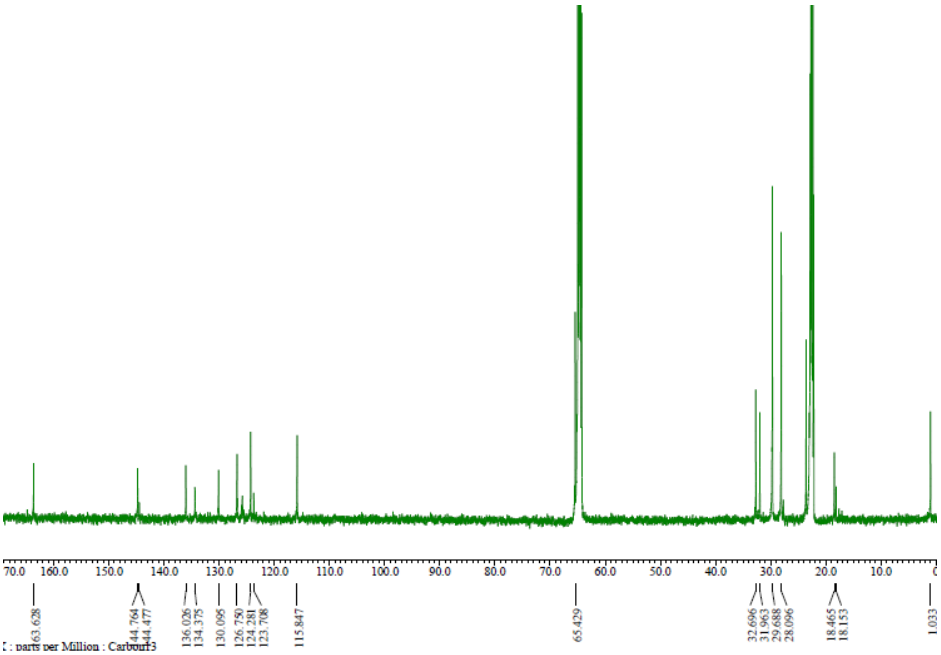

Fig. S9 ^{1}H NMR spectrum of **6** in THF-d_8.

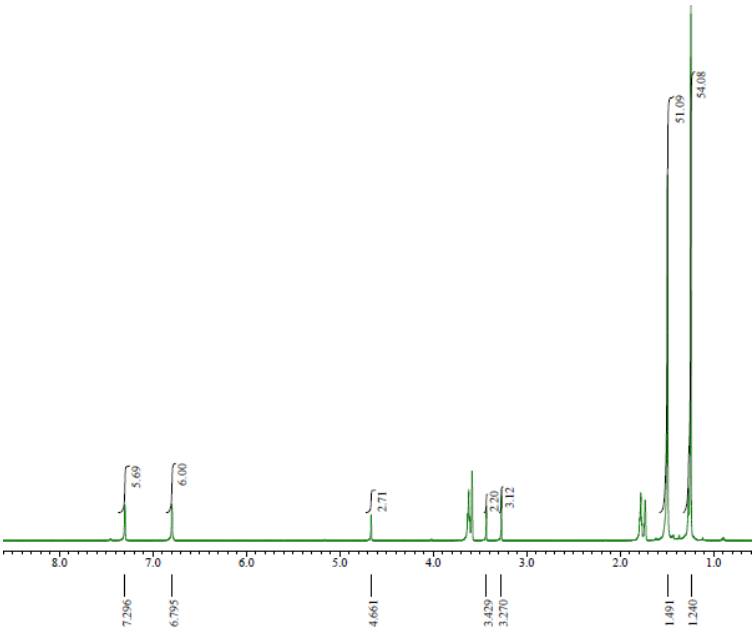

Fig. S10 ^{13}C{^{1}H} NMR spectrum of **6** in THF-d_8.

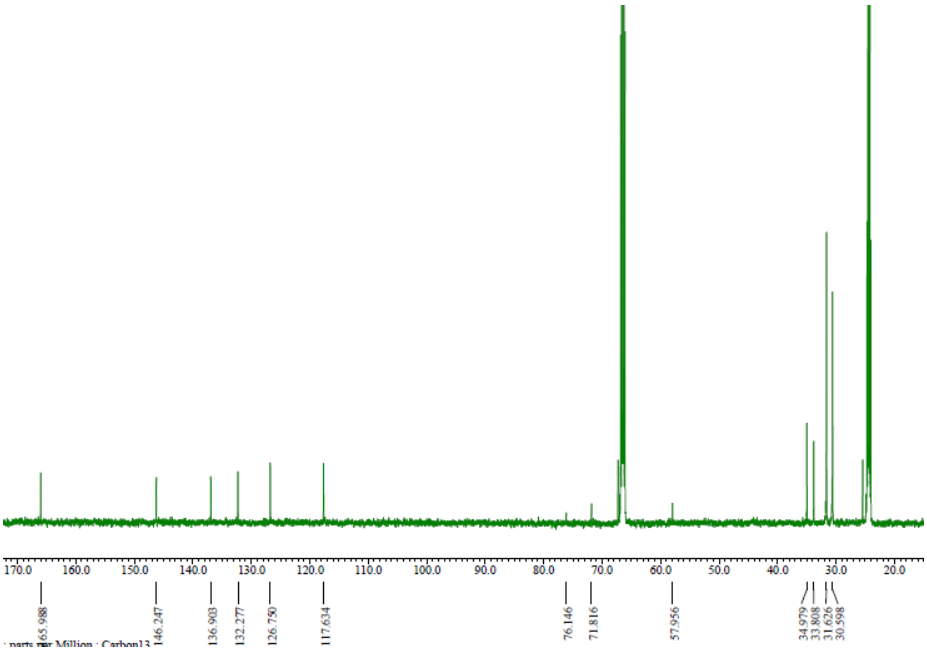

Fig. S11 ^{1}H NMR spectrum of $[K_2(thf)_2(O_3C)Zr(CH_2Ph)_2]$ in THF-d_8.

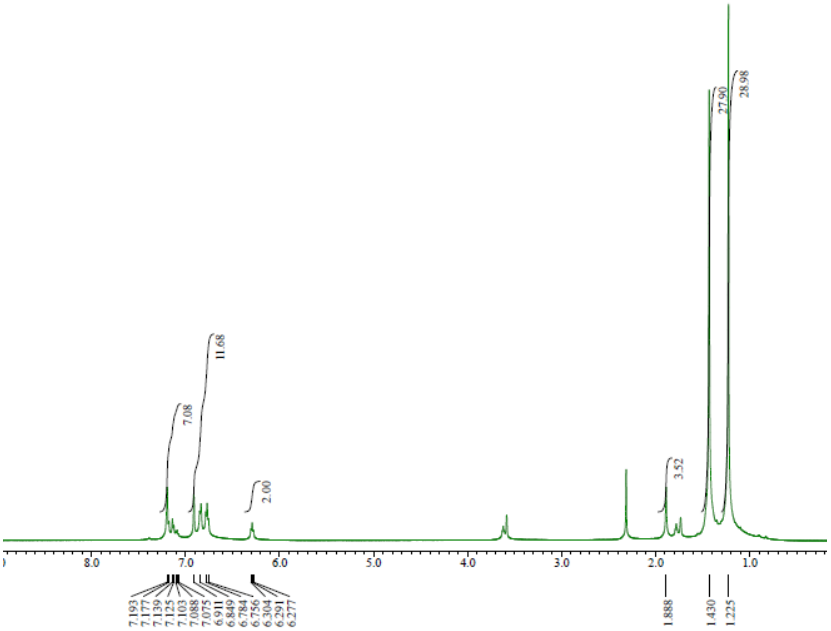

Fig. S12 ^{13}C{^{1}H} NMR spectrum of $[K_2(thf)_2(O_3C)Zr(CH_2Ph)_2]$ in THF-d_8.

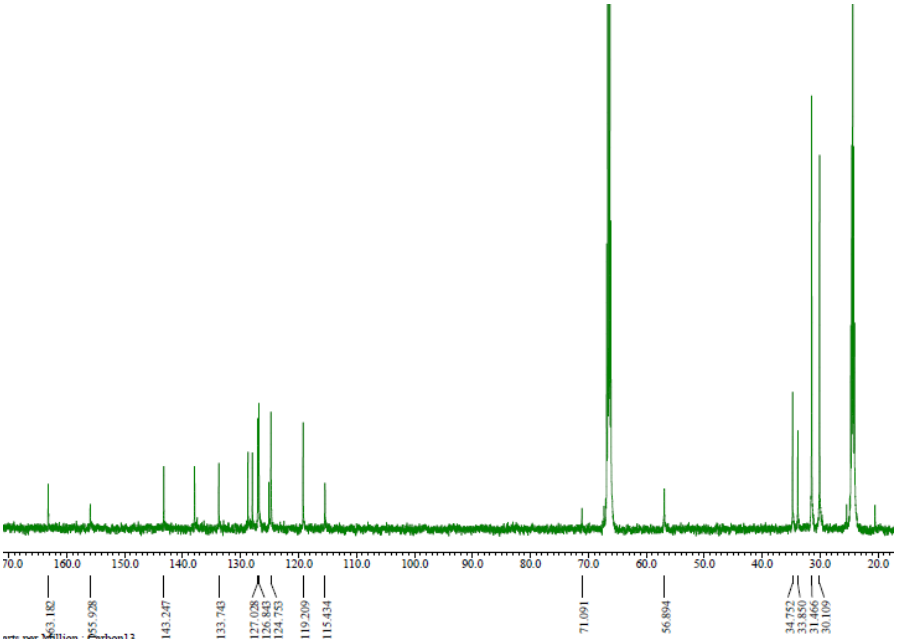

Fig. S13 ^{1}H NMR spectrum of the reaction mixture of **2** with one equiv of Me_3SiN_3 after 1 h. The peaks at ca. 6.5–8.0 ppm are shown below.

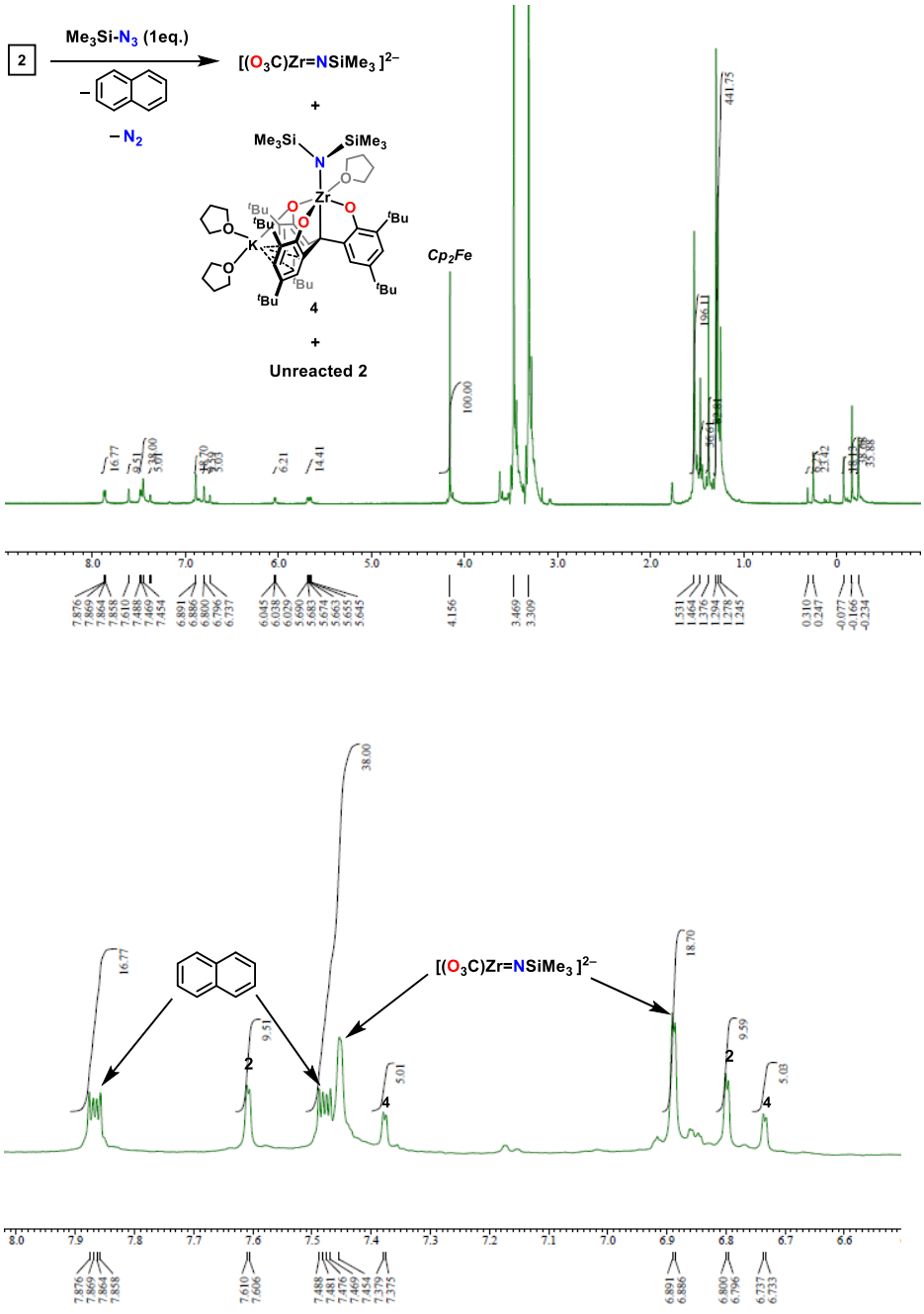

Fig. S14 ^{1}H NMR spectrum of the reaction mixture of **2** with one equiv of $MesN_3$ after 1 h.

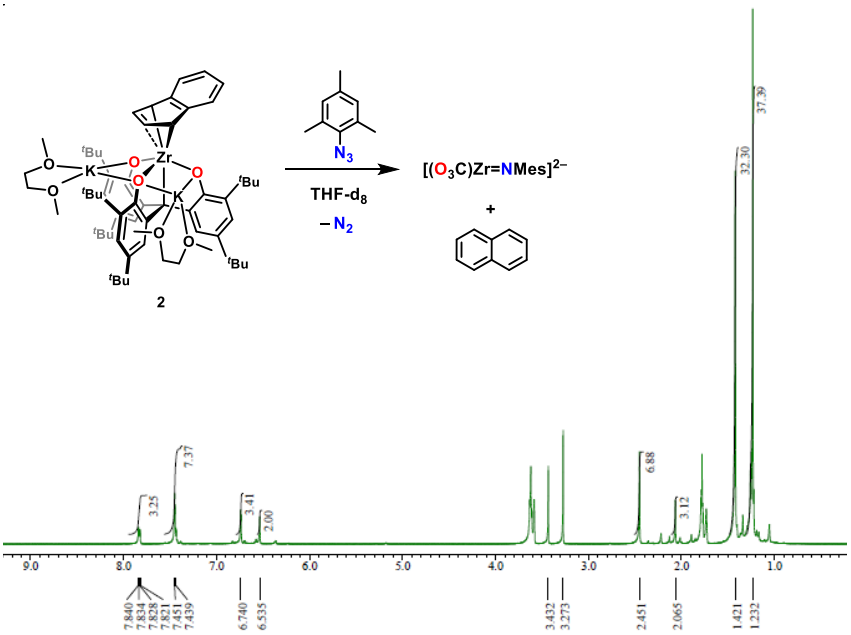

Fig. S15 ^{1}H NMR spectrum of the reaction mixture of **2** with H_2 in THF-d_8 after 72 h.

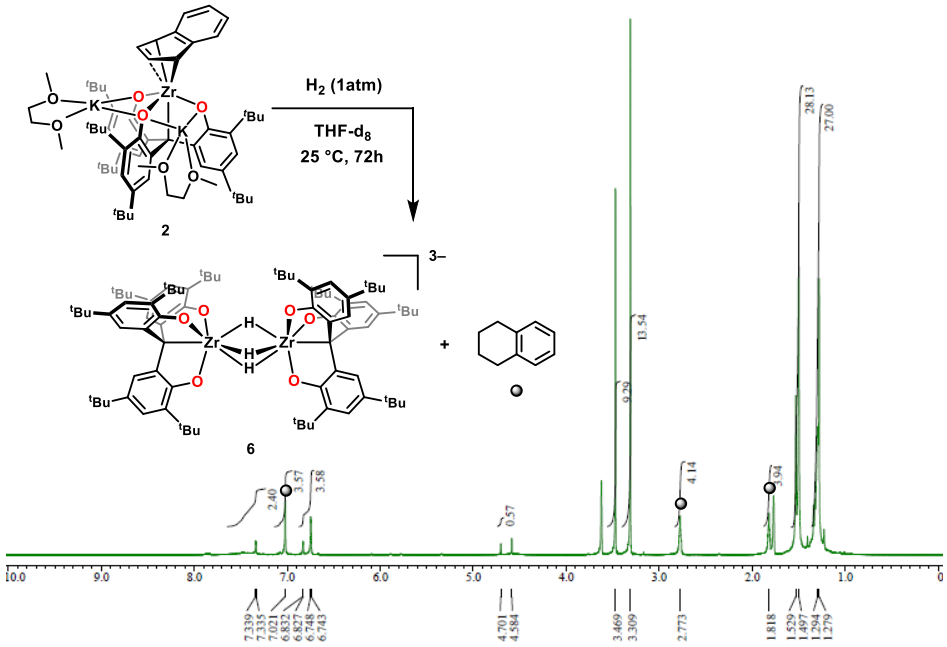

Fig. S16 Structure of **4** with thermal ellipsoids set at 30% probability level. Selected bond lengths [Å] and angles [°]: Zr(1)–O(1) 2.082(2), Zr(1)–O(2) 2.093(3), Zr(1)–O(3) 2.054(2), Zr(1)–O(4) 2.329(2), Zr(1)–C(1) 2.322(3), Zr(1)–N(1) 2.180(3), O(1)–Zr(1)–O(2) 135.56(9), O(2)–Zr(1)–O(3) 112.52(9), O(3)–Zr(1)–O(1) 89.40(9), Zr(1)–N(1)–Si(1) 118.27(14), Si(1)–N(1)–Si(2) 119.83(16), Si(2)–N(1)–Zr(1) 121.07(15).

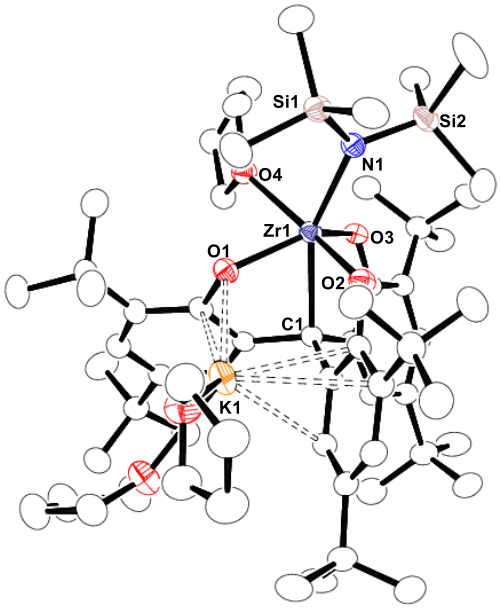

Fig. S17 Molecular structure of the benzyl complex $[K_2(thf)_2(O_3C)Zr(CH_2Ph)_2]$ with thermal ellipsoids set at 30% probability level. Only one of two independent moleucles in the asymmetric units is shown. All hydrogen atoms are omitted for clarity. Selected bond lengths [Å] and angles [°]: Zr(1)-O(1) 2.202(3), Zr(1)-O(2) 2.308(3), Zr(1)–O(3) 2.113(3), Zr(1)–C(1) 2.308(3), Zr(1)–C(2) 2.382(5), Zr(1)–C(3) 2.356(5), Zr(1)···C(46) 3.390(4), Zr(1)···C(52) 3.343(4), O(1)–Zr(1)–O(2) 97.47(11), O(2)–Zr(1)–O(3) 146.34(12), O(3)–Zr(1)–O(1) 88.53(11), Zr(1)–C(2)–O(46) 121.6(3), Zr(1)–C(3)–C(52) 119.9(3).

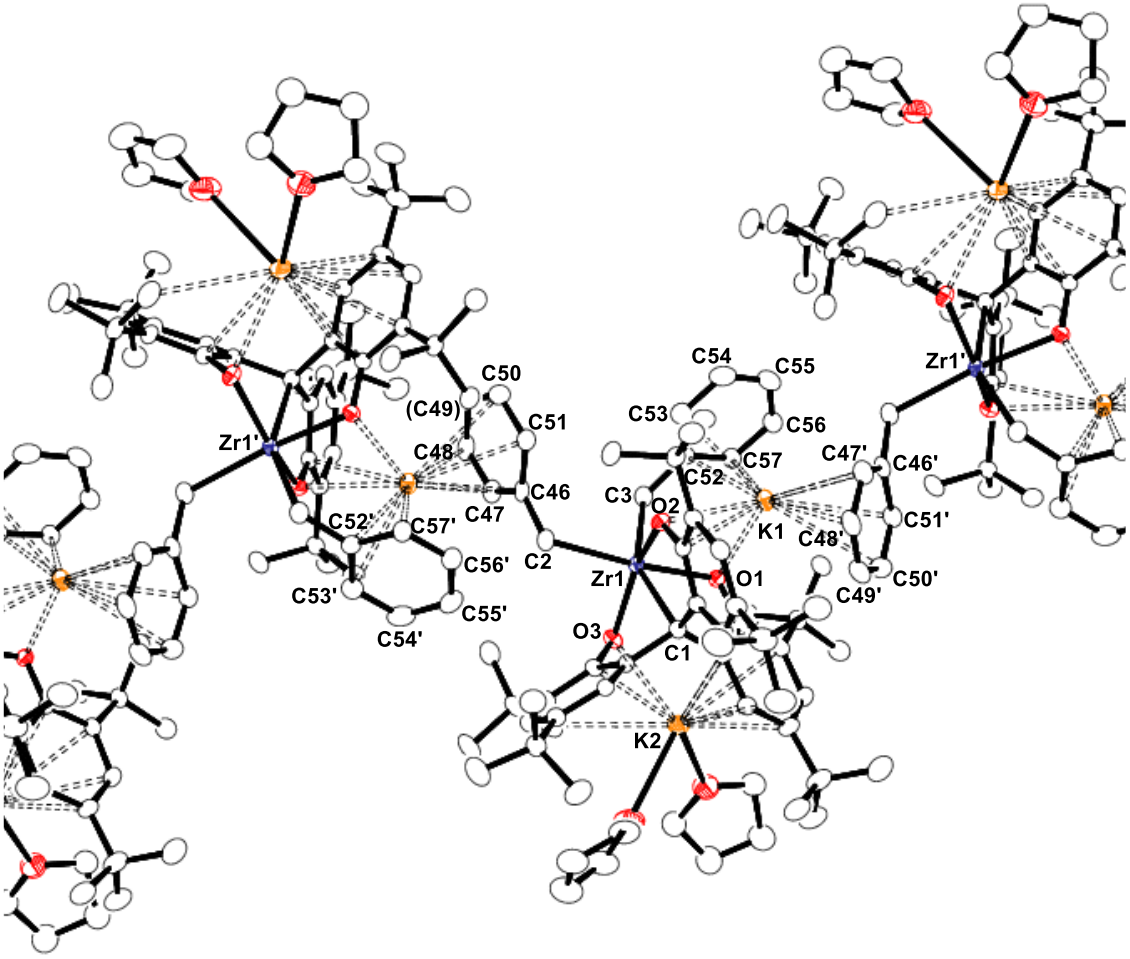

Table S1 Crystallographic data for **2**, **4**, **5**, and $[K_2(thf)_2(O_3C)Zr(CH_2Ph)_2]$.

Crystal Data for **2**	
formula	$C_{61}H_{88}K_2O_7Zr$
mol wt(g mol^{-1})	1102.73
T (K)	123(2)
crystal system	orthorombic
space group	$P2_12_12_1$ (#19)
crystal color	Brown
crystal size (mm)	0.36 × 0.11 × 0.08
Solvent	DME/hexane
a (Å)	16.976(3)
b (Å)	17.780(3)
c (Å)	20.404(4)
α (deg)	90
β (deg)	90
γ (deg)	90
V ($Å^3$)	6158.6(19)
Z	4
ρ_{calc} (g cm^{-3})	1.189
μ (Mo Kα) (cm^{-1})	0.361
Abs. Correction type	Multi-scan
Abs. Transmission (min/max)	0.9105/1.0000
$2\theta_{max}$ (deg)	54.9
no. of reflections collected	51412
no. of unique reflections (R_{int})	14001 (0.0549)
R_1 [I > 2σ(I)] [a]	0.0531
wR_2 (all data) [b]	0.1228
Goodness of fit on F^2	1.117
Largest diff. peak and hole/e $Å^{-3}$	0.593 and –0.706 e·$Å^{-3}$

(a) $R_1 = \Sigma||F_o|-|F_c|| / \Sigma|F_o|$, (b) $wR_2 = [\Sigma\{w(F_o^2-F_c^2)^2\} / \Sigma\{w(F_o^2)^2\}]^{0.5}$

Table S1 Crystallographic data for **2**, **4**, **5**, and $[K_2(thf)_2(O_3C)Zr(CH_2Ph)_2]$. (Cont.)

Crystal Data for **4**	
formula	$C_{61}H_{102}KNO_6Si_2Zr\bullet(C_5H_{12})$
mol wt(g mol^{-1})	1204.08
T (K)	123(2)
crystal system	monoclinic
space group	$P2_1/n$ (#4)
crystal color	Yellow
crystal size (mm)	0.25 × 0.23 × 0.17
Solvent	pentane
a (Å)	18.5178(9)
b (Å)	17.2279(7)
c (Å)	22.3406(10)
α (deg)	90
β (deg)	92.825(3)
γ (deg)	90
V ($Å^3$)	7118.5(6)
Z	4
ρ_{calc} (g cm^{-3})	1.124
μ (Mo Kα) (cm^{-1})	0.291
Abs. Correction type	Multi-scan
Abs. Transmission (min/max)	0.9105/1.0000
$2\theta_{max}$ (deg)	54.9
no. of reflections collected	72124
no. of unique reflections (R_{int})	16217 (0.0532)
R_1 [I > 2σ(I)] [a]	0.0748
wR_2 (all data) [b]	0.2727
Goodness of fit on F^2	1.010
Largest diff. peak and hole/e $Å^{-3}$	2.518 and –1.051 e·$Å^{-3}$

(a) $R_1 = \Sigma||F_o|-|F_c|| / \Sigma|F_o|$, (b) $wR_2 = [\Sigma\{w(F_o^2-F_c^2)^2\} / \Sigma\{w(F_o^2)^2\}]^{0.5}$

Table S1 Crystallographic data for **2**, **4**, **5**, and $[K_2(thf)_2(O_3C)Zr(CH_2Ph)_2]$. (Cont.)

Crystal Data for **5**	
formula	$C_{67}H_{104}KNO_6SiZr$, $0.5(C_{10}H_8)$
mol wt(g mol^{-1})	1242.00
T (K)	123(2)
crystal system	monoclinic
space group	$C2/c$ (#15)
crystal color	Yellow
crystal size (mm)	0.19 × 0.13 × 0.12
Solvent	pentane
a (Å)	47.946(13)
b (Å)	14.776(4)
c (Å)	20.070(5)
α (deg)	90
β (deg)	96.033(3)
γ (deg)	90
V ($Å^3$)	14140(6)
Z	8
ρ_{calc} (g cm^{-3})	1.167
μ (Mo Kα) (cm^{-1})	0.279
Abs. Correction type	Multi-scan
Abs. Transmission (min/max)	0.9105/1.0000
$2\theta_{max}$ (deg)	54.9
no. of reflections collected	82629
no. of unique reflections (R_{int})	16156 (0.0829)
R_1 [I > $2\sigma(I)$] [a]	0.0728
wR_2 (all data) [b]	0.2371
Goodness of fit on F^2	1.041
Largest diff. peak and hole/e $Å^{-3}$	1.114 and –0.814 e·$Å^{-3}$

(a) $R_1 = \Sigma||F_o|-|F_c|| / \Sigma|F_o|$, (b) $wR_2 = [\Sigma\{w(F_o^2-F_c^2)^2\} / \Sigma\{w(F_o^2)^2\}]^{0.5}$

Table S1 Crystallographic data for **2**, **4**, **5**, and $[K_2(thf)_2(O_3C)Zr(CH_2Ph)_2]$. (Cont.)

Crystal Data for $[K_2(thf)_2(O_3C)Zr(CH_2Ph)_2]$	
formula	$C_{65}H_{90}K_2O_5Zr$, 0.5(C_5H_{12}), 0.5(C_4H_8O)
mol wt(g mol^{-1})	1192.91
T (K)	123(2)
crystal system	monoclinic
space group	$P2_1/n$ (#14)
crystal color	Yellow
crystal size (mm)	0.20 × 0.18 × 0.16
Solvent	pentane/THF
a (Å)	22.405(4)
b (Å)	17.330(3)
c (Å)	35.658(7)
α (deg)	90
β (deg)	95.581(2)
γ (deg)	90
V ($Å^3$)	40865(3)
Z	8
ρ_{calc} (g cm^{-3})	1.150
μ (Mo Kα) (cm^{-1})	0.326
Abs. Correction type	Multi-scan
Abs. Transmission (min/max)	0.9105/1.0000
$2\theta_{max}$ (deg)	54.9
no. of reflections collected	148879
no. of unique reflections (R_{int})	31474 (0.0694)
R_1 [I > $2\sigma(I)$] [a]	0.893
wR_2 (all data) [b]	0.2563
Goodness of fit on F^2	0.950
Largest diff. peak and hole/e $Å^{-3}$	1.484 and –0.675 e·$Å^{-3}$

(a) $R_1 = \Sigma||F_o|-|F_c|| / \Sigma|F_o|$, (b) $wR_2 = [\Sigma\{w(F_o^2-F_c^2)^2\} / \Sigma\{w(F_o^2)^2\}]^{0.5}$